RSC Advances

A Unique Fabrication Strategy of Hierarchical Morphologies: Combination of Multi-Step Self-Assembling and Morphology Transition

Journal:	*RSC Advances*
Manuscript ID:	RA-ART-03-2015-005105.R1
Article Type:	Paper
Date Submitted by the Author:	23-Apr-2015
Complete List of Authors:	Pan, Cai-Yuan ; University of Science and Technology of China, Department of Polymer Science and Engineering Zhang, Wen-Jian; University of Science and Technology of China, Department of Polymer Science and Engineering Hong, Chun-Yan; University of Science and Technology of China, Department of Polymer Science and Engineering

Table of Contents

A Unique Fabrication Strategy of Hierarchical Morphologies: Combination of Multi-Step Self-Assembling and Morphology Transition

Wen-Jian Zhang, Chun-Yan Hong, Cai-Yuan Pan**

CAS Key Laboratory of Soft Matter Chemistry, Department of Polymer Science and Engineering, University of Science and Technology of China, Hefei, Anhui, 230026, P. R. China.

E-mail: hongcy@ustc.edu.cn, pcy@ustc.edu.cn

Sea cucumber-like hierarchical microstructures were fabricated, and a multi-step self-assembling process was observed in the RAFT dispersion polymerization.

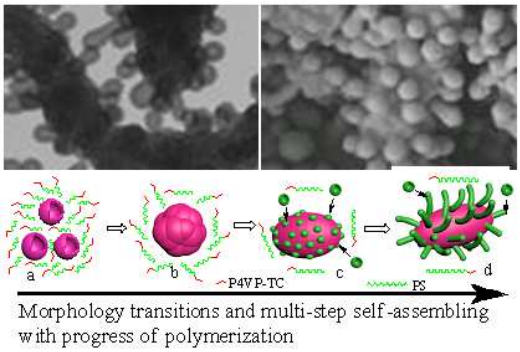

Cite this: DOI: 10.1039/c0xx00000x

www.rsc.org/xxxxxx

ARTICLE TYPE

A Unique Fabrication Strategy of Hierarchical Morphologies: Combination of Multi-Step Self-Assembling and Morphology Transition

Wen-Jian Zhang, Chun-Yan Hong,* Cai-Yuan Pan*

Received (in XXX, XXX) Xth XXXXXXXXX 20XX, Accepted Xth XXXXXXXXX 20XX

DOI: 10.1039/b000000x

Abstract: Multi-compartmental cylindrical microstructures with lots of nanotubes on their surface, whose shape resembles sea cucumber, have been fabricated for the first time. This hierarchical morphology is formed through transitions of vesicles to large compound vesicles, to sea cucumber-like hierarchical microstructures. Along with the morphology transitions, aggregation of the residual polymer chains in the solution occurs, which is called as multi-step self-assembling. The driving force of the phase transitions and the multistep self-assembling is polymerization because with progress of the polymerization, the chain length ratio of PS to P4VP increases, which induces self-assembling and morphology transition. The requisite for multi-step self-assembling is high concentration of the P4VP-PS chains remained in the solution after formation of the nascent assemblies. The concentration of the residual block chains can be controlled by varying recipe and content of the ethanol. Thus, this study provides a unique strategy to fabricate useful hierarchical assemblies.

Introduction

Polymeric solid or hollow spheres with hierarchical surface structures, especially in shape of the fruits or the sea fishes, have attracted great attention because of unusual shape and high surface area, which make them very useful for applications in various fields, such as drug delivery, catalysis, and inorganic templates.[1] Among such morphologies, the most studied morphologies are snowman-like and raspberry-like microspheres, which are generally prepared by seeded emulsion polymerization.[2] Other important strategy for fabrication of such hierarchically structured particles is removal of the solvent from oil-in-water emulsion droplets, leading to formation of various morphologies including rambutanlike microspheres, which was induced by hydrodynamic instability of the interface between organic solvent droplets and water.[3] Using flow-focusing in a microcapillary device to generate solvent droplets with uniform size in water, microspheres with surface coated with "budding" vesicles were formed.[4] Compare to the morphologies formed from block vinyl polymers, rigid polymers, such as polyanilines (PANs), can generate more morphologies. Rambutan-like hollow PAN microspheres were prepared by oxidation polymerization of aniline in the presence of perfluorooctane sulfonic acid.[5] By change of solvent, dopant, oxidant/monomer ratio, temperature, various morphologies including urchinlike, dandelion-like and rambutan-like spheres were formed in oxidation polymerization of anilines, the driving force was various molecular interactions, such as hydrogen bonding, π–π stacking, and van der Waals interactions.[6]

Performance of the polymeric nanoparticles is strongly affected by their morphologies.[7] For example, cylindrically-shaped filomicelles persisted in the blood circulation for up to one week after intravenous injection, which is much longer than their spherical counterparts.[7c] Thus, studying cylindrical micelles with hierarchical surface structures is of practical importance also. Although canonical structures of spherical micelles, cylindrical micelles and vesicles,[8] and a myriad of more complex assemblies including toroids, Janus structures, large compound micelles, tubes, large compound vesicles, and multilayer vesicles, etc have been fabricated either by self-assembling strategy or directly from polymerization,[9] the multi-compartmental cylindrical microstructures with lots of short nanotubes on their surface, whose shape resembles sea cucumber, have not been prepared. How can this type of assemblies be fabricated? In this article, the sea cucumber-like morphologies are successfully fabricated for the first time, and through this fabrication, we tried to explore basic principle for fabricating the assemblies with hierarchical structure in the controlled free radical polymerizations.

Generally, encapsulation, or coagulation and fusion of two different assemblies in the same system can produce some interesting morphologies,[2,10] for example, rambutan-like particles were prepared in a seeded emulsion polymerization by attaching small sized aggregates onto the large spherical particles.[2] Thus, after the nascent assemblies are formed, the block copolymer chains remained in the polymerization solution can self-assemble continuously, which is called as multi-step self-assembling in this study, to afford the small sized assemblies or different morphologies of the assemblies, and then the two different assemblies are agglomerate and fused, some interesting assemblies are fabricated, one of them is sea cucumber-like

assemblies. However, this multi-step self-assembling is very difficult to achieve because concentration of the residual block copolymer after formation of the nascent aggregates is generally too low to self-assemble again.[10a] Therefore, a crucial problem for multi-step self-assembling is how to control concentration of the residual polymer chains in a dispersion polymerization system, which was never reported in the previous publications based on our knowledge.

Experimental Section

Materials

4-Vinylpyridine (4VP, Acros, 96%) was dried over CaH_2, then distilled under reduced pressure prior to use. N, N'-azobis(isobutyronitrile) (AIBN) was purified by recrystallization from ethanol. Styrene (St, Shanghai Chem. Co. >99%) was washed with an aqueous solution of sodium hydroxide (5 wt%) three times and then washed with distilled water until neutralization. After being dried with anhydrous magnesium sulfate, St was distilled under reduced pressure. S-1-dodecyl-S-(α,α'-dimethyl-α''-acetic acid)trithiocarbonate (TC) was synthesized according to our previous report.[10c] All other reagents were of analytical grade and were used as received.

Synthesis of TC-terminated Poly(4-vinylpyridine) (P4VP-TC)

The general procedure is as follows. 4VP (6.0 g, 57.14 mmol), TC (218 mg, 0.60 mmol), AIBN (10 mg, 0.06 mmol) and isopropanol (5 mL) were added into a 20 mL polymerization tube with a magnetic bar. After three freeze-evacuate-thaw cycles, the tube was sealed under high vacuum, and then the sealed tube was placed in an oil bath at 80 °C while stirring for 3.5 h. After cooling to room temperature, the polymer solution was diluted with CH_2Cl_2 and then poured into excess petroleum ether while stirring. The precipitate was collected by filtration and then dried in a vacuum oven at room temperature. The yellow solid was dissolved in CH_2Cl_2, and the precipitation procedure was repeated three times. The resultant product was dried under vacuum at room temperature overnight.

Fabrication of sea cucumer-liked hierarchical microstructures by RAFT dispersion polymerization

The P4VP-TC (11 mg, 2.5×10^{-3} mmol) mixed with AIBN (0.042 mg, 2.5×10^{-4} mmol) and various amount of St and ethanol (for feed molar ratio of P4VP-TC/St/ethanol = 20000/1/0.1, 5.2 g of St and 3.0, or 3.6, or 4.2, or 4.8 g of ethanol; for the ratio =15000/1/0.1, 3.9 g of St, 2.25, or 2.70, or 3.15, or 3.60 g of ethanol; for the ratio =10000/1/0.1, 2.60 g of St, 1.50, or 1.80, or 2.10, or 2.40 g of ethanol) were added in a glass tube with a magnetic bar, and then the system was degassed by three freeze-pump-thaw cycles. The tube was sealed under vacuum, and then the sealed tubes were placed in an oil bath at 80 °C for predetermined time while stirring.

Measurements of the P4VP-PS remained in the solution after polymerization for different time

P4VP-TC (11 mg, 2.5×10^{-3} mmol), AIBN (0.042 mg, 2.5×10^{-4} mmol), St (5.2 g, 50 mmol) and ethanol (4.8 g) were respectively added into four glass tubes with magnetic bars, and then the systems were degassed by three freeze-pump-thaw cycles. The tubes were sealed under vacuum, and then the sealed tubes were placed in an oil bath at 80 °C while stirring for 12 h, 24 h, 36 h and 48 h, respectively. The reaction mixtures were poured into four centrifuge tubes and kept in a water bath at 80 °C for 30 min, respectively. The formed aggregates were deposited on the bottom of the centrifuge tubes and 3.0 g of the supernatant liquid were taken out from the four tubes, respectively. The supernatant liquids were kept under vacuum for several days to remove most of the ethanol and unreacted styrene. Then 0.3 g tetrahydrofuran (THF) were added into the residuals, respectively. The THF solutions were taken for ^{1}H NMR characterization. The content of molecule-soluble P4VP-PS in the 3.0 g reaction media can be calculated according to the ^{1}H NMR.

Measurements of the P4VP-PS remained in the solution after polymerization with various ratios of ethanol/St for 24 h

The P4VP-TC (11 mg, 2.5×10^{-3} mmol) was mixed with AIBN (0.042 mg, 2.5×10^{-4} mmol) and St (5.2 g, 50 mmol), and various amount of ethanol (4.0 g, 4.2 g, 4.4 g, 4.6 g and 4.8 g) in glass tubes with magnetic bars, and then the systems were degassed by three freeze-pump-thaw cycles. The tubes were sealed under vacuum, and then the sealed tubes were placed in an oil bath at 80°C while stirring for 24 h. Then the reaction mixtures were poured into five centrifuge tubes, and kept in a water bath at 80°C for 30 min. The formed aggregates were deposited on the bottom of the centrifuge tubes and 3.0 g of the supernatant liquid were taken out of the five samples, respectively. The supernatant liquids were kept under vacuum for several days to remove most of the ethanol and unreacted styrene. Then 0.3 g tetrahydrofuran (THF) were added into the residuals, respectively. The THF solutions were taken for ^{1}H NMR characterization. The content of P4VP-PS in 3.0 g of the reaction media can be calculated based on the ^{1}H NMR data.

The relationship of monomer conversion and DPPS with the feed molar ratio of St/P4VP-TC

St (1.73 g, 16.67 mmol) and ethanol (1.6 g) were mixed with various amounts of P4VP-TC and AIBN (the molar ratio of P4VP-TC/AIBN was 5/1 for all the samples and the molar ratios of St/P4VP-TC were changed from 50 to 20000) in glass tubes with magnetic bars, and then the systems were degassed by three freeze-pump-thaw cycles. The tubes were sealed under vacuum, and then the sealed tubes were placed in an oil bath at 80°C while stirring for 36 h. The reaction mixtures were cooled to room temperature quickly, and the mixtures were taken for ^{1}H NMR characterization directly. The monomer conversions were calculated according to the integral values ratio of the St to ethanol proton signals before and after the polymerization (the content of the ethanol in the reaction systems were quantitative). The DP_{PS}s herein were calculated according to the monomer conversions and the initial molar ratios of St/P4VP-TC.

Characterization

The ^{1}H NMR (300 MHz) measurements were performed on Bruker DMX300 spectrometer in $CDCl_3$ using tetramethylsilane as an internal reference. The molecular weight and molecular weight distribution of the P4VP were determined by gel-permeation chromatography (GPC), using four Styragel columns (HR1, HR3, HR4, and HR5) at 60°C and a Waters 2414

differential refractive index (RI) detector at 40°C; DMF was utilized as the eluent at a flow rate of 1 mL/min. The molecular weight and molecular weight distribution of the P4VP-PS were determined on a Waters 150C gel permeation chromatography (GPC) equipped with three ultrastyragel columns (500, 10^3, 10^4Å) in series and RI 2414 detector at 30 °C, and THF was used as eluent at a flow rate of 1.0 mL/min. Monodispersed polystyrene standards were used in the calibration of molecular weight and molecular weight distribution. The transmission electron microscope (TEM) observations were performed on a Hitachi H-800 TEM at an accelerating voltage of 100 kV. The samples for TEM observations were prepared by depositing a drop of the nanoparticle dispersion in ethanol on copper grids. The fieldemission scanning electron microscope (FESEM) images were measured on a JEOL JSM-6700F. The samples were prepared by placing a drop of the nanoparticle dispersion in ethanol on copper grids, and gilding a shell of Pt nanoparticle.

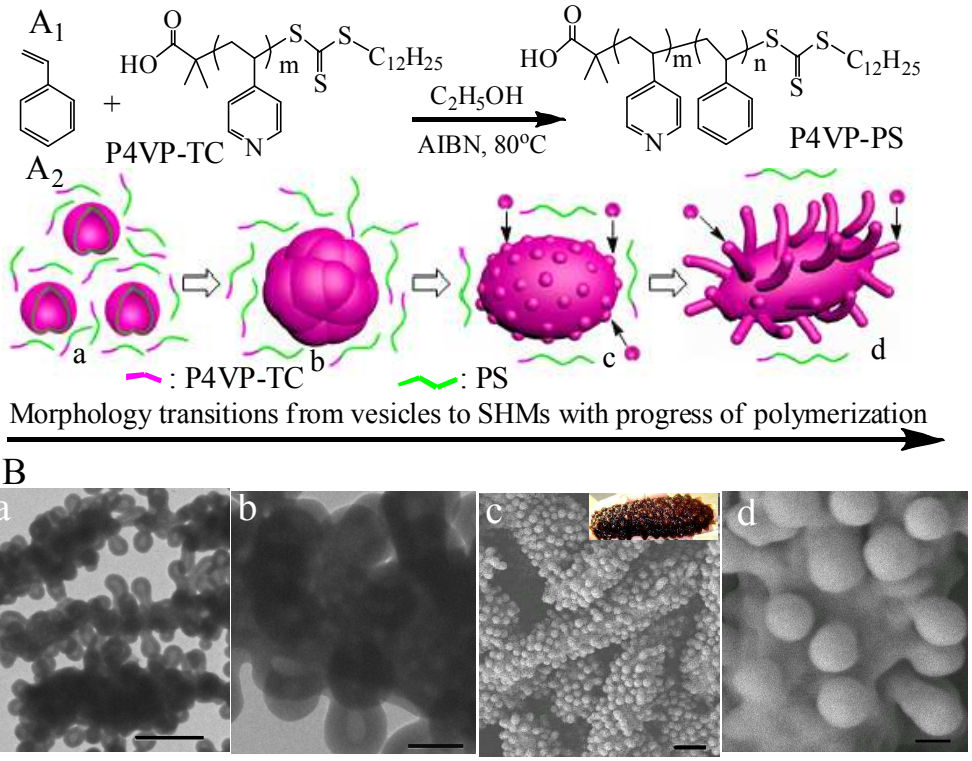

Fig. 1 Formation of sea cucumber-like hierarchical microstructures in the RAFT dispersion polymerization. A_1: Schematic polymerization reactions and A_2: morphology transitions from vesicles to sea cucumber-like hierarchical microstructures (SHMs) in the RAFT dispersion polymerization. B: TEM (a, b) and SEM images (c, d) of the assemblies fabricated in RAFT dispersion polymerization with a feed molar ratio of St/$P4VP_{39}$/AIBN = 20000/1/0.1 in ethanol (ethanol/St = 0.7/1, w/w) at 80 °C for 36 h. Inserting picture of c is a digital photo of sea cucumber. Scale bars for a and c are 1 μm; scale bars for b and d are 200 nm.

Results and Discussion

In order to explore the basic principle for fabrication of the sea cucumber-like morphology, the system we selected is the RAFT dispersion polymerization of styrene (St) using poly(4-vinylpyridine) (P4VP) as both macro-RAFT agent and stabilizer. The block copolymer synthesis is shown in Fig. $1A_1$. The P4VP-TC was synthesized by the RAFT polymerization of 4VP in 2-propanol at 80 °C for 3.5 h using s-1-dodecyl-S-(α,α'-dimethyl-α''-acetic acid)trithiocarbonate (TC) as RAFT agent. Nearly monodispersed P4VP-TC with M_n = 5700, M_w/M_n = 1.09, which was estimated by GPC (Fig. S1), was obtained, and its ^{1}H NMR spectrum in Fig. S2 shows characteristic proton signals of P4VP at δ = 8.29, 6.34, 2.48 and 1.39 ppm, as well as the proton signals of TC at δ = 3.23, 1.21 and 0.83 ppm. The number-average degree of polymerization (DP = 39) was calculated based on the integration ratio of the signal at δ = 6.34, to that at δ = 3.23 ppm. This $P4VP_{39}$-TC was used in the subsequent study.

Fabrication of sea cucumber-like hierarchical microstructures

Based on description in introduction, fabrication of the sea cucumber-like assemblies requires a polymerization system, in which the multi-step self-assembling occurs. Thus, relatively high concentration of the residual copolymer chains after formation of the large aggregates is essential to actualize this purpose. Similar to precipitation fractionation that the polymers with different molecular weights can be separated based on the amount of the precipitators added, in a dispersion polymerization system, the nature and dosage of a selective solvent also influence concentration of the residual polymers in the solution. In this study, ethanol was selected as a selective solvent instead of methanol we usually used because the ethanol has a lower

solubility parameter (δ = 26.0) than the methanol (δ = 29.7), and its δ is more close to the δ of PS (δ = 16.6-20.3).[11] In addition, the St is a good solvent of the PS, with the conversion increase, its content in the mixture of ethanol/St decreases, leading to decrease of the residual polymer chains in the solution. When the conversion is high, less St remain in the solution, and all the block copolymer chains may be aggregated. Thus, controlling the conversion of St is important for preparation of sea cucumber-like assemblies. Based on our studies on the RAFT dispersion polymerization of St using P4VP as Macro RAFT agent, the conversion of St significantly decreases with the feed molar ratio increase of St/P4VP, which will be discussed later. In order to enhance the residual block copolymer concentration, a high feed molar ratio of St/P4VP39 ($r_{St/P4VP}$)=20000/1 was used. For fabrication of sea cucumber-like assemblies, we referenced our previous studies on the fabrication of large compound vesicles (LCV) also,[12] a RAFT dispersion polymerization with a feed molar ratio= 20000/1/0.1 in ethanol (C_2H_5OH/St = 0.7/1, w/w) at 80°C was designed to use in the following studies besides special mention.

To identify whether this polymerization system can produce the sea cucumber-like hierarchical microstructures (SHMs), the TEM and FESEM were respectively applied to observe morphologies of the assemblies obtained. A TEM image of the resultant assemblies in Fig. 1Ba displays cylindrical hierarchical microstructures with lots of short nanotubes on their surface, the cylindrical hierarchical microstructures have broad distributions in both their lengths and diameters (Ds), the longest can be up to 8 μm, and the Ds are between 0.4 ~ 1.0 μm. All nanotubes on the surface are closed and most of them are capped with a half ball, their sizes are small relative to their cylindrical microparticles, their Ds and lengths are around 200 nm and 400~650 nm, respectively. The compartmental structure of the cylindrical hierarchical microstructures can be clearly seen in Fig. 1Bb, demonstrating high porosity and large inner superficial area of the SHMs formed. Their FESEM image in Fig. 1Bc reveals many cylinders on surface of the large cylindrical micelles, and their shape resembles the sea cucumber as shown in the inserting digital photo of Fig. 1Bc. Fig. 1Bd shows that the surface of cylindrical hierarchical microstructures is not smooth, but coarse besides the protrudent nanotubes. We refer the multicompartmental cylindrical microstructures with lots of nanotubes on their surface as SHMs.

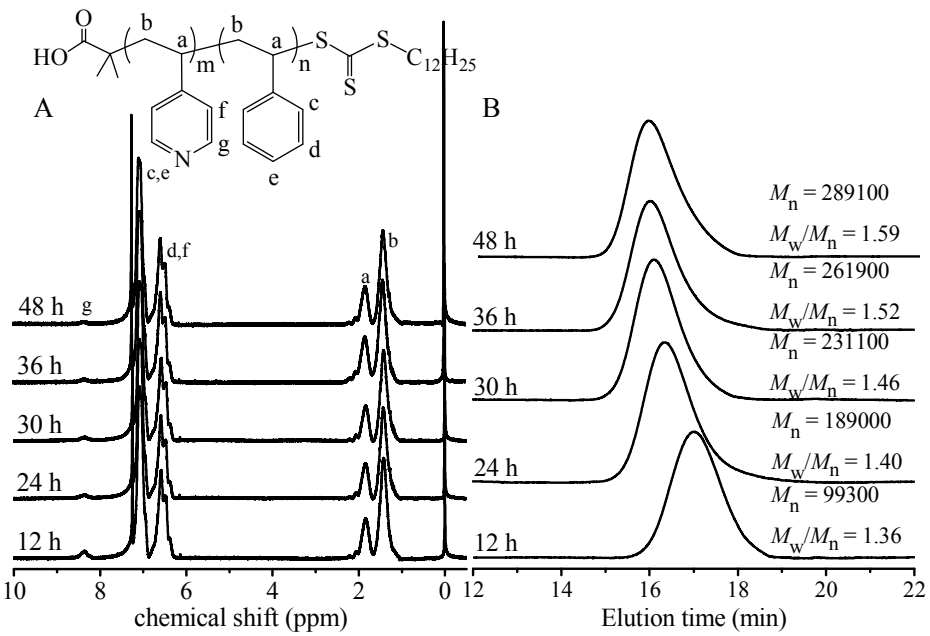

Fig. 2 ^{1}H NMR spectra (A, in $CDCl_3$) and GPC traces (B) of the block copolymers, $P4VP_{37}$-PS_m formed in the RAFT dispersion polymerization at 80°C with feed molar ratio of St/P4VP/AIBN = 20000/1/0.1 in ethanol (ethanol/St = 0.7/1) for different polymerization time.

Formation process of the SHMs

As description in previous publications,[12] when the amphiphilic block copolymer chains in the vesicles became highly asymmetric, the interfacial tension led the vesicles to coagulation and fusion, forming the LCV, in these studies, the assemblies with hierarchical surface structures have not been reported. However, the polymerization system herein is able to fabricate SHMs. To answer why the present system can, but the previous reported system cannot fabricate SHMs, clarifying formation mechanism of the SHMs is necessary. Therefore, the ^{1}H NMR, GPC, TEM and FESEM were used to follow the polymerization, the ^{1}H NMR spectra and GPC traces, the TEM and FESEM images of the resultant assemblies at different polymerization time are respectively shown in Fig. 2 and Fig. 3. Based on these results, we proposed a formation process of the SHMs as shown in Fig. 1A_2.

As we expected, the RAFT polymerization of St using P4VP as Macro RAFT agent produces a block copolymers, PS-P4VP,

which is supported by the ^{1}H NMR spectra of the resultant polymers obtained at different polymerization time in Fig. 2A: the characteristic signals of pyridyl protons in the 4VP units at δ = 8.36 ppm (g) and phenyl protons in the St units at δ = 7.05 ppm (c and e). The DPs of PS blocks were calculated based on the integral values of the above two signals and M_n(NMR) of the P4VP. The results are listed in Table S1. We can see that with progress of the polymerization, the DPs of PS blocks increase significantly, 970 at 12h and 3420 at 48h. The GPC traces in the Fig. 2B reveals similar results, and the M_ns of the PS-P4VP are significantly enhanced with progress of the polymerization: 99300 g/mol at 12h and 289100 g/mol at 48h.

As reported in previous studies,[8, 12] the morphology is strongly determined by the chain length ratio (R) of the hydrophobic to hydrophilic blocks. In the RAFT dispersion polymerization, the PS block grew to a critical chain length, self-assembling occurred to form spherical micelles at first. Continuous polymerization in the spheres induced the morphology transitions from spheres to rods, and then to vesicles.[12] Fig. 3 shows changes of the morphology with R variation of the block copolymers formed. Similar to the previous studies,[12] when the PS-P4VP chains grow to DP_{PS} = 970 (R = 24.9), the vesicles are formed, and their TEM image in Fig. 3A reveals that all assemblies are vesicles with a D of approximately 340 nm and a wall thickness of ~68 nm. Continuous growth of the P4VP-PS chains in the wall of vesicles leads to R increase, and when the R reaches to 56.9, coagulation and fusion of the vesicles occur, forming the spherical LCVs (Fig. 1A$_2$b), their multi-compartmental structure can be clearly seen in the TEM image of Fig. 3B, and a few of pits on surface of the LCV in their FESEM image of Fig. 3B' demonstrate the existence of cavities in the inner of assemblies. Different from very slow growth rate of the PS-P4VP chains in methanol after formation of the LCV,[12] the PS-P4VP chains in the LCVs grow relatively fast (Fig. 5A) in comparison with the methanol used as selective solvent probably owing to high concentration of the un-reacted St. When the R increases from 56.9 to 71.5, the LCVs are coagulated and fused to form cylindrical hierarchical microstructures with lots of bulges on their surface as shown in Fig. 1A$_2$c, Fig. 3C and 3C'. The inserting picture of Fig. 3C is magnification of the micelle in the red rectangle, and we can see that the bulges are formed by coagulating the vesicles with D of ~160 nm and wall thickness of ~60 nm, which are smaller than the smallest vesicles in Fig. 3A and 3A'demonstrating that they are produced after formation of the vesicles in Fig. 3A. Thus, it is reasonable to speculate that the bulges on the surface of cylindrical particles are formed through coagulation and fusion of the small vesicles formed by self-assembling of the residual PS-P4VP chains in the solution. Since their concentration in the solution is relatively low, formation of the smaller vesicles is reasonable.

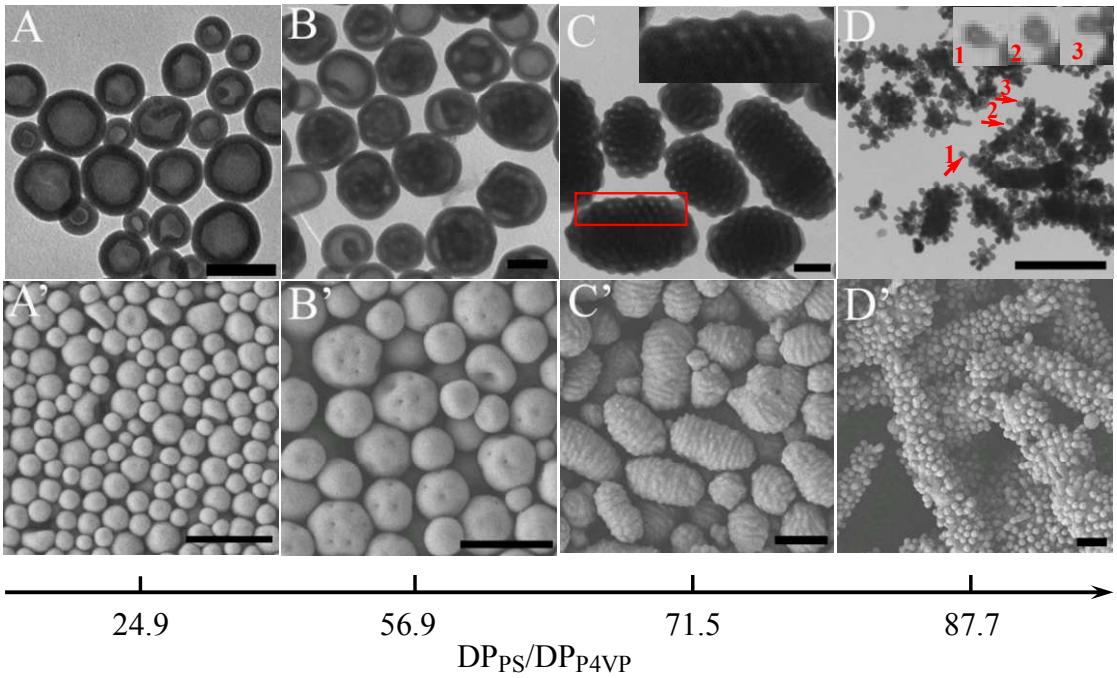

Fig. 3 Formation process of the sea cucumber-like hierarchical microstructures. TEM images (A~D) and FESEM images (A'~D') of the aggregates obtained from the polymerization for 12 h (A and A'); 24 h (B and B'); 30 h (C and C'); 48 h (D and D'); the scale bars are 400 nm for A, B and C, 4 μm for D. The scale bars for A' ~D' are 1 μm. All aggregates were fabricated from RAFT dispersion polymerization at 80°C with feed molar ratio of St/P4VP$_{39}$/AIBN = 20000/1/0.1 in ethanol (ethanol/St=0.7/1, w/w).

As aforementioned, there are a lot of protrudent nanotubes on surface of the SHMs as shown in Fig. 1Ba. From the FESEM images in Fig. 3C' and 3D' respectively acquired at 30 h and 48h of polymerization, the short nanotubes on surface of the SHMs come obviously from growth of the bulges. How are the short nanotubes formed? There are two possible formation processes: one is precipitation of the high molecular weight PS-P4VP chains in the solution to the assemblies existed; other is self-assembling of the growing residual PS-P4VP chains to form vesicles first, and then coagulation of the vesicles to the assemblies existed. We

did not observe the evidence for the former process, but the evidence of the latter process was observed. Carefully analyzing the TEM image in Fig. 3D, we can understand the entire formation process of these nanotubes. When the PS-P4VP chains in the small residual polymer chains vesicles continuously grow to high DP, such as DP_{PS} = 3420 (R = 87.7), the vesicles become unstable and are coagulated to the protrudent part of the bulges on surface of the cylindrical microstructures as shown in the part pointed by the red arrow 1, which is similar to assembling of the polymer aggregates in solution.[13] Subsequently, the vesicle and the bulge on the surface start to fuse through rearrangement of the polymer chains, but the fusion is not completed, we can see the protrudent nanotube capped with a big ball as shown in the red arrow 2. After the fusion is completed, a short nanotube capped with a half ball is observed as shown in the red arrow 3. Summarily, the protrudent nanotubes on surface of the SHMs are formed through coagulation-fusion process of the newly formed vesicles, therefore, progressive formation of the vesicles by multi-step self-assembling is essential for success of nanotubes formation.

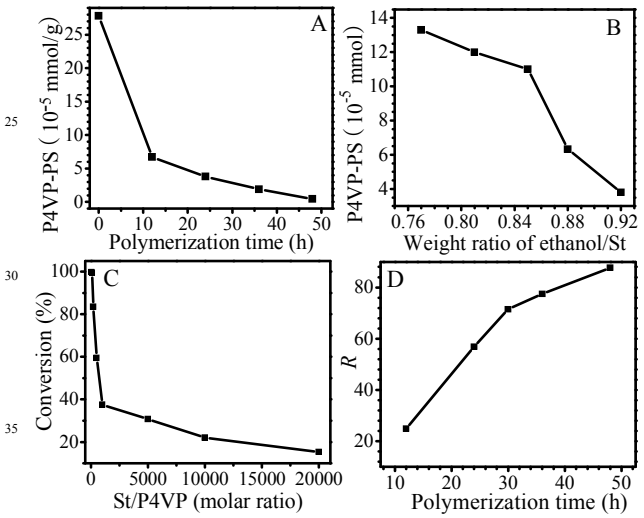

Fig. 4 Influencing factors for fabrication of sea cucumber-like hierarchical microstructures. (A) Concentration of the residual PS-P4VP chains in reaction media with progress of polymerization; (B) Effect of the weight ratio of ethanol/St on amount of the residual P4VP-PS in the media; (C) Effect of St/P4VP (molar ratio in feed) on conversion of the St for 36 h of polymerization; (D) Relationship of chain length ratio of PS to P4VP with polymerization time. All data were obtained from the RAFT dispersion polymerization in ethanol at 80°C; feed molar ratio of $St/P4VP_{39}/AIBN$ = 20000/1/0.1 for A, B and D; ethanol/St = 0.7/1 (w/w) for D, 0.92/1 (w/w) for A and C; polymerization time: 24h for B.

Influencing Factors for Formation of SHMs

From formation process of the SHMs described above, we know that chain growth of the PS-P4VP in the assemblies and in the solution respectively induce morphology transitions of the vesicles to the spherical LCVs, to the cylindrical LCVs and self-assembling to form the small sized vesicles and then short nanotubes. To clarify why the morphology transitions and the self-assembling can be taken place in the same polymerization system and then further understand the formation mechanism of SHMs, it is necessary to study distribution of the PS-P4VP chains between the assemblies and solution and the chain growth rate or molecular weight increase rate of the PS-P4VP. Therefore, ^1H NMR was used to estimate the concentrations of PS-P4VP chains remained in the solution, and the results are shown in Fig. 4A. When the polymerization was carried out for 12 h, the vesicles were formed and approximately 24% of the initial P4VP-PS chains with concentration of 6.7×10^{-5} mmol/g remained in the solution and approximately 76% of the initial PS-P4VP chains formed vesicles. Comparatively, for the RAFT dispersion polymerization in methanol, only approximately 1% of the initial P4VP-PS chains remained in the solution at formation of the nascent vesicles.[10a] With progress of the polymerization, the residual PS-P4VP chains in the solution decreased gradually, and at 48h of polymerization, the residual polymer concentration is 4.3×10^{-6} mmol/g, which is only 1.5% of the initial PS-P4VP chains owing to continuous formation of the small sized vesicles via self-assembling.

Similar to the influencing factors for formation of the morphologies,[8a] one of the important factors for controlling concentration of the residual PS-P4VP chains is nature and composition of the solvents. In a RAFT dispersion polymerization of St in ethanol, the polymerization media is a mixture of ethanol and St, their relative ratio significantly influences the residual PS-P4VP chains in the solution. When the polymerization was carried out in various weight ratios of ethanol/St for 24h, the concentration of PS-P4VP remained in the solution was measured, and the results are shown in Fig. 4B. With increasing weight ratio of the ethanol/St, the concentrations of residual PS-P4VP chains in solution decrease, for example, 13.3×10^{-5} mmol/g at weight ratio of ethanol/St =0.77 and 3.8×10^{-5} mmol/g at 0.92 of ethanol/St. This is easier understandable because St is a good solvent; ethanol is a precipitator of the PS, increasing the content of St generally enhances solubility of the PS-P4VP chains in the polymerization media. Thus, the dosage of ethanol is an important factor influencing the concentration of PS-P4VP chains remained in solution, and further influencing the formation of SHMs. Besides the reaction media, other important influencing factor is the feed molar ratio of St/P4VP ($r_{St/P4VP}$). We studied relationship between the conversion of St and the $r_{St/P4VP}$, the results are shown in Fig. 4C. The conversion of St is greatly dependent on the feed molar ratio of St/P4VP, and the monomer conversion decreases with increasing the feed molar ratio of St/P4VP. So, at high $r_{St/P4VP}$, more monomer St remains in the solution at formation of the vesicles. Consider only 1.5% of the initial PS-P4VP chains remained in the mixture of ethanol/St when the weight ratio of ethanol/St=0.92/1 was used, high $r_{St/P4VP}$ (such as 20000/1, molar ratio) and less ethanol (such as ethanol/St=0.7/1, wt/wt) were used for fabrication of SHMs.

As we know, self-assembling of the PS-P4VP chains must lead to decrease of their concentration in the solution; their further self-assembling requires higher critical chain length, or larger chain length ratio of PS/P4VP than the previous self-assembling of the polymer chains, so, a question is, can the residual PS-P4VP chains grow to so high R? Fig. 4D reveals that after 30h of polymerization, the R increase is not as fast as that before the

formation of LCVs, but the R increases still fast with progress of the polymerization because the St concentration in the media changes slightly (relative content of St decreased from 58 wt% at formation of the vesicles to 54 wt% at formation of the SHMs).

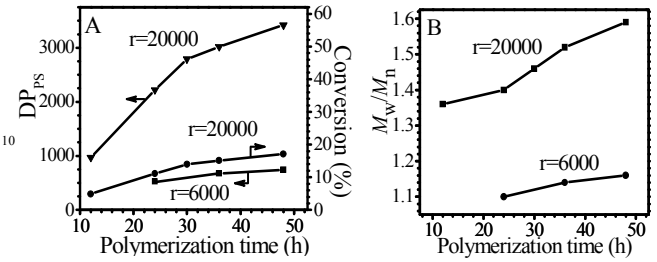

Fig. 5 Influence of molar ratio of St/P4VP on polymerization rate, chain growth rate and molecular weight of the resultant PS-P4VP. A: DP increase of the PS block and St conversion with progress of polymerization; B: The influence of polymerization time on molecular weight distribution. Polymerizations with a feed molar ratio of $St/P4VP_{39}$/AIBN=20000/1/0.1 and 6000/1/0.1 were performed in ethanol (ethanol/St=0.7/1, w/w) at 80 ^{o}C.

At high feed molar ratio of St/P4VP, the polymerization rate is relatively slow, but the chain growth rate is quite fast. We respectively measured chain lengths of the PS block and the monomer conversions with different polymerization time, and the results are shown in Fig. 5A. We can see that the polymerization rate is slow, but the chain growth rate is quite fast, which is reasonable when we consider each chain radical consumes a lot of monomer molecules, but total amount of the St consumed by less residual chains is still low. The feed molar ratio of St/P4VP not only affects the residual PS-P4VP chains, but also affects the chain growth rate. For the polymerization with $r_{St/P4VP}$=6000, the chain growth rate is much slower than that for the polymerization with $r_{St/P4VP}$=20000 as shown in Fig. 5A, which is understandable because the concentration of un-reacted St is much lower (Fig.4C). Owing to low residual PS-P4VP chains in the solution and low chain growth rate, the polymerization with $r_{St/P4VP}$ =6000 produced only the vesicles.

When the residual PS-P4VP chains cannot be neglected after formation of the assemblies, the polymerizations in the aggregates and in the solution should be considered. Theoretically, the chain growth rate of the P4VP-PS in the aggregates is restricted by diffusion of St in the solution to the aggregates. For the polymerization with $r_{St/P4VP}$=20000, the chain growth rate in the assemblies should be lower than that in the solution, so, the PS-P4VP chains growing in the solution have higher DP than that growing in the assemblies. Thus, we observe an interesting phenomenon that the polydispersity indexes of the resultant PS-P4VP increase with progress of the polymerization (Fig. 5B). However, for the polymerization with $r_{St/P4VP}$=6000, the molecular weight distributions are narrow and the polydispersity indexes are slightly changed with progress of the polymerization as shown in Fig. 5B because the concentration of residual PS-P4VP chains is too low to self-assemble, so, they are not coagulated to the solid assemblies.

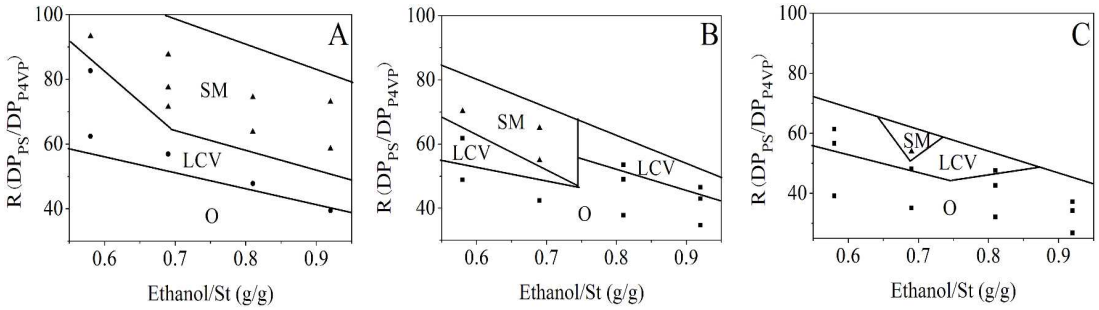

Fig. 6 Recipe and conditions for fabrication of SHMs in RAFT dispersion polymerization at 80^{o}C. Detailed phase diagram was drew based on the results of polymerization with the feed molar ratios of $St/P4VP_{39}$/AIBN = 20000/1/0.1 (A); 15000/1/0.1 (B); 10000/1/0.1 (C). SHM = sea cucumber-like hierarchical microstructures, LCV = large compound vesicles, O = vesicles and nanowires.

Recipe and Conditions for Fabrication of SHMs

Above discussion demonstrates that the $r_{PS-P4VP}$, nature and dosage of the ethanol are significant factors for fabrication of the SHMs. To further understand how the factors affect the formation of SHMs, we studied formation of the assemblies under various recipes and dosage of the ethanol, their GPC traces and TEM images are shown in Fig. S3 and S4, and the results are summarized in Fig. 6 and Table S1.

As shown in Fig. 6A, when the polymerization with $r_{St/P4VP}$ = 20000 was carried out in various contents of ethanol for 24 h, no SHMs, but vesicles or LCVs were fabricated. However, after the polymerization in the ethanol/St=0.68, 0.81 and 0.92 (wt/wt) was carried out for 36h, the R values respectively reached to 77.5, 63.8 and 58.6, the SHMs were fabricated. For the polymerization in ethanol/St = 0.58 (wt/wt), owing to relatively high solubility of the P4VP-PS in the media, self-assembling requires high critical chain length of the PS block, so, no SHMs, but the LCVs were formed although the R value reached to 82.7, and the formation of SHMs was achieved until R=93.3. With decrease of the $r_{St/P4VP}$ from 20000 to 10000, the chain growth rates decreased, the weight ratio range of ethanol/St for fabrication of the SHMs became narrow. When the $r_{St/P4VP}$ equals to 15000, only the polymerizations in the mixture of ethanol/St = 0.58 (wt/wt) for 48h and 0.68 for 36 h and 48 h, the SHMs were fabricated as shown in Fig. 6B, and for the ethanol/St ratios of 0.81 and 0.92, no SHMs were fabricated owing to low concentration of the residual copolymer chains in the solution (Fig. 4B). For the

$r_{St/P4VP}$=10000, the SHMs were achieved only for the polymerization in the mixture of ethanol/St=0.68 (wt/wt) for 48h (Fig. 6C). All these results further support that the $r_{St/P4VP}$ and the ethanol dosage are important factors for preparation of the SHMs.

Conclusions

In summary, the multi-compartmental cylindrical microstructures with lots of short nanotubes on their surface have been successfully fabricated by RAFT dispersion polymerization. Different from the canonical morphologies fabricated via one-step self-assembling and morphology transition, this special morphology is formed via combination of morphology transition and multi-step self-assembling. A crucial point for achieving this purpose is high concentration of the P4VP-PS remained in the solution after formation of the nascent aggregates, which is determined by feed molar ratio of St/P4VP, nature and dosage of the solvent.

Acknowledgment

This work is supported by the National Natural Science Foundation of China under contract No. 21074121, 21090354, 21374107, China Postdoctoral Science Foundation (BH2060000011) and the Fundamental Research Funds for the Central Universities (WK 2060200012).

Notes and references

Key Laboratory of Soft Matter Chemistry, Chinese Academy of Sciences, Department of Polymer Science and Engineering, University of Science and Technology of China, Hefei, Anhui, 230026, P. R. China.
E-mail: hongcy@ustc.edu.cn, pcy@ustc.edu.cn
†Electronic Supplementary Information (ESI) available: [Characterization of the polymers and the aggregates obtained (Fig. S1 to S4) are included in the supporting information.]. See DOI: 10.1039/b000000x/

1 (a) F. Caruso, *Adv. Mater*. 2001, **13**, 11–22; (b) Y. Wang, M. S. Hassan, P. Gunawan, R. Lau, X. Wang, R. J. Xu, *Colloid Interface Sci.* 2009, **339**, 69–77; (c) J. S. Lee, J. Feijen, *J. Control. Release* 2012, **161**, 473–483; (d) E. S. Lee, K. T. Oh, D. Kim, Y. S. Youn, Y. H. Bae, *J. Control. Release* 2007, **123**, 19–26; (e) D. M. Vriezema, P. M. L. Garcia, N. S. Oltra, N. S. Hatzakis, S. M. Kuiper, R. J. M. Nolte, A. E. Rowan, J. C. M. van Hest, *Angew. Chem. Int. Ed.* 2007, **46**, 7378–7382; (f) W. J. Zhang, C. Y. Hong, C. Y. Pan, *J. Mater. Chem. A*, 2014, **2**, 7819-7828.

2 (a) A. Perro, S. Reculusa, E. Bourgeat-Lami, E. Duguet, S. Ravaine, *Colloids Surf. A*, 2006, **284–285**, 78–83; (b) S. Shi, S. Kurodab, K. Hosoi, H. Kubota, *Polymer* 2005, **46**, 3567–3570; (c) G. Yang, Y. Liu, R. Jia, R. Xu, X. Wang, L. Ling, J. Yang, *J. Appl. Polym. Sci.* 2009, **112**, 410–415.

3 (a) J. Zhu, R. C. Hayward, *J. Am. Chem. Soc.* 2008, **130**, 7496–7502; (b) J. Zhu, N. Ferrer, R. C. Hayward, *Soft Matter* 2009, **5**, 2471–2478.

4 J. Zhu, R. C. Hayward, *Angew. Chem. Int. Ed.* 2008, **47**, 2113 –2116.

5 Y. Zhu, D. Hu, M. Wan, L. Jiang, Y. Wei, *Adv. Mater.* 2007, **19**, 2092–2096.

6 (a) J. Wang, J. Wang, Z. Wang, F. Zhang, *Macromol. Rapid Commun.* 2009, **30**, 604–608; (b) T. Guo, F. Liao, Z. Wang, S. Yang, *J. Mater. Sci. Res.* 2012, **1**, 25–30; (c) Q. Lü, C. Wang, X. Cheng, *Microchim Acta* 2010, **169**, 233–239.

7 (a) J. M. Dean, N. E. Verghese, H. Q. Pham, F. S. Bates, *Macromolecules* 2003, **36**, 9267–9270; (b) J. M. Dean, R. B. Grubbs, W. Saad, R. F. Cook, F. S. Bates, *J. Polym. Sci. Part B-Polym. Phys.* 2003, **41**, 2444–2456; (c) Y. Geng, P. Dalhaimer, S. S. Cai, R. Tsai, M. Tewari, T. Minko, D. E. Discher, *Nature Nanotechnology*, 2007, **2**, 249–255.

8 (a) Y. S. Yu, A. Eisenberg, *J. Am. Chem. Soc.* 1997, **119**, 8383–8384; (b) T. Azzam, A. Eisenberg, *Angew. Chem.-Int. Ed.* 2006, **45**, 7443–7447; (c) S. Sugihara, A. Blanazs, S. P. Armes, A. J. Ryan, A. L. Lewis, *J. Am. Chem. Soc.* 2011, **133**, 15707–15713; (d) Y. Li, S. P. Armes, *Angew. Chem.-Int. Ed.* 2010, **49**, 4042–4046; (e) W. M. Wan, X. L. Sun, C. Y. Pan, *Macromolecules* 2009, **42**, 4950–4952; (f) E. Groison, S. Brusseau, F. D'Agosto, S. Magnet, R. Inoubli, L. Couvreur, B. Charleux, *ACS Macro Lett.* 2012, **1**, 47−51; (g) W. M. Wan, C. Y. Hong, C. Y. Pan, *Chem. Comm.* 2009, 5883-5885.

9 (a) A. Blanazs, J. Madsen, G. Battaglia, A. J. Ryan, S. P. Armes, *J. Am. Chem. Soc.* 2011, **133**, 16581–16587; (b) P. Zou, C. Y. Pan, *Macromol. Rapid Commun.* 2008, **29**, 763–771; (c) W. M. Wan, C. Y. Pan, *Polym. Chem.* 2010, **1**, 1475–1484; (d) R. Erhardt, M. Zhang, A. Böker, H. Zettl, C. Abetz, P. Frederik, G. Krausch, V. Abetz, A. H. E. Müller, *J. Am. Chem. Soc.* 2003, **125**, 3260–3267.

10 (a) W. J. Zhang, C. Y. Hong, C. Y. Pan, *Macromolecules* 2014, **47**, 1664-1671; (b) H. Shen, A. Eisenberg, *Angew. Chem. Int. Ed.* 2000, **39**, 3310–3312; (c) W. M. Wan, C. Y. Pan, *Macromolecules* 2010, **43**, 2672–2675.

11 J. Brandrup, E. H. Immergut, E. A. Grulke, *Polymer handbook*, New York, Wiley-Interscience, 4th edn, 1999, vol. 3, p. VII699–VII701, VII711.

12 (a) W. M. Cai, W. M. Wan, C. Y. Hong, C. Q. Huang, C. Y. Pan, *Soft Matter* 2010, **6**, 5554–5561; (b) J. T. Sun, C. Y. Hong, C. Y. Pan, *Soft Matter* 2012, **8**, 7753–7767; (c) W. M. Wan, X. L. Sun, C. Y. Pan, *Macromol. Rapid Commun.* 2010, **31**, 399–404.

13 (a) C. Q. Huang, C. Y. Pan, *Chinese J. Polym. Sci.* 2008, **26**, 341–352; (b) Y. Wang, Z. Liu, B. Han, J. Li, H. Gao, J. Wang, J. Zhang, *J. Phys. Chem. B* 2005, **109**, 2605–2609.